



**DUTCH-BELGIAN BEAMLINE
AT ESRF**

**EUROPEAN
SYNCHROTRON
RADIATION FACILITY**



Experiment Report Form

Instructions for preparing your Report

- fill in a separate form for each project or series of measurements.
- type your report, in English.
- include the reference number of the proposal to which the report refers.
- make sure that the text, tables and figures fit into the space available.
- if your work is published or is in press, you may prefer to paste in the abstract, and add full reference details. If the abstract is in a language other than English, please include an English translation.

(next page)



	Experiment title: Dynamic diffraction in colloidal crystals	Experiment number: 26-02-166
Beamline: BM-26B DUBBLE	Date(s) of experiment: From: 14-07-2003 To: 18-07-2003	Date of report: - -2003
Shifts: 9	Local contact(s): Igor Dolbnya	
Names and affiliations of applicants (* indicates experimentalists): A.V. Petoukhov*, D.G.A.L. Aarts*, X. Xian*, G.J. Vroege, H.N.W. Lekkerkerker (van 't Hoff lab, Utrecht), I. Dolbnya* (DUBBLE CRG/ESRF)		

Report: (max. 2 pages)

The present experiment was devoted to dynamic effects [1] in small-angle x-ray diffraction (SAXD) in long-range-ordered [2] hard-sphere colloidal crystals. Diffraction was recorded at 8 metres distance from the sample by a CCD detector (pixel size 25 μm). The sample description and further experimental details can be found elsewhere [1-3].

During the experiment the SAXD patterns were measured from the same crystals using $E = 25$ keV and $E = 10$ keV x-rays. The idea behind these measurements was to vary the refractive index contrast $\delta n \propto 1/E^2$ and, thus, the relative intensity of the diffracted waves, $I_{(hkl)} \propto (\delta n)^2 \propto 1/E^4$, where hkl denote the usual Miller indices of reflections. While at $E = 10$ keV diffraction was expected to be deep into the dynamic regime [1,3], at 25 keV we anticipated (nearly) kinematic diffraction. Figure 1 presents examples of our measurements at these two energies. The bright diffraction features originate from the stacking-independent $(hk0)$ Bragg spots with $h-k$ divisible by 3 [1-3]. Weaker reflections originating from Bragg rods can also be seen. The patterns at the two energies E are collected at different exposure times (to compensate for the limited dynamic range of the detector [3]) and for various crystal orientations. The collected data require a somewhat cumbersome numerical analysis and further theoretical modelling, which will be performed later. In the following we focus on another aspect, the resolving power, which could be of interest for other users of the BM-26B SAXS/WAXS station.

Figure 2 presents examples of horizontal intensity profiles $I(q_x)$ through particular reflections. The dots present detector readings per pixel while the solid lines are Gaussian fits $I(q_x) = A \exp(-q_x^2/2\sigma^2) + I_0$, where A is the peak height, q_x is the wave vector mismatch, σ is the standard deviation and I_0 is the detector offset. All reflections measured at both energies are found to have the same width $2\sigma = 5.15 \pm 0.1$ detector pixels, or about 120 μm in the detector plane. In reciprocal space, this corresponds to an apparent reflection width 2σ of 2 μm^{-1} and 0.8 μm^{-1} for 25 and 10 keV x-

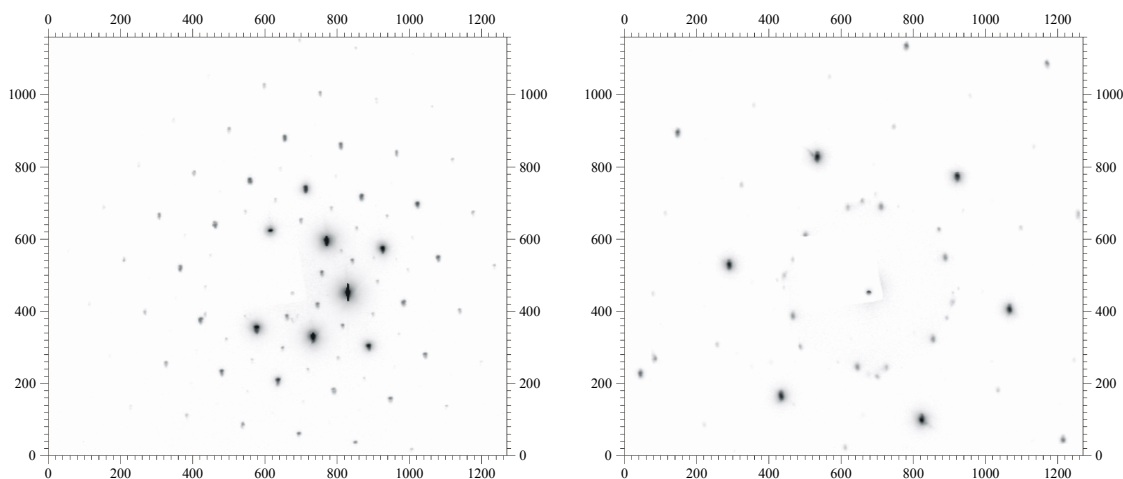


Fig. 1 Diffraction pattern of the same crystal measured with 25 keV (left) and 10 keV (right) x-rays.

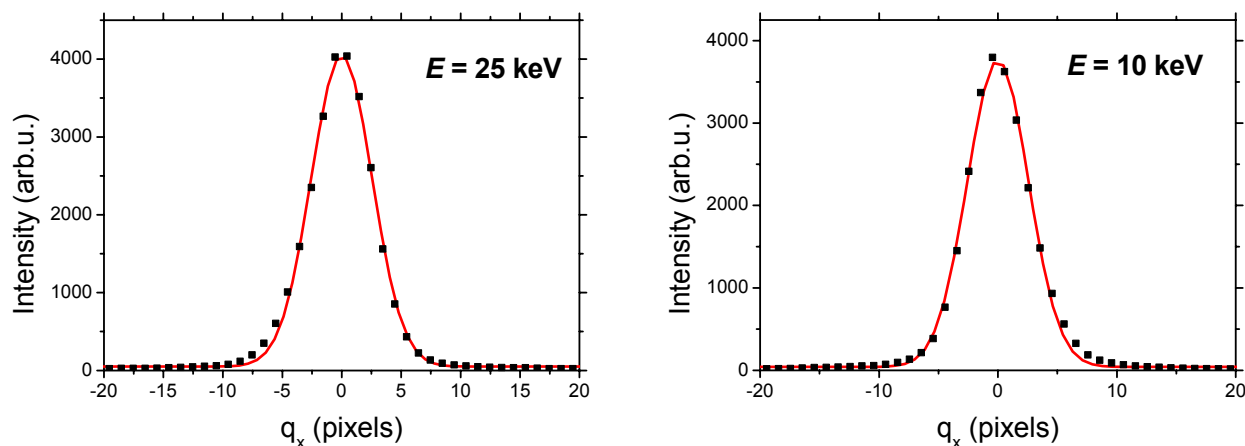


Figure 2. Horizontal profile through two particular reflections in the diffraction patterns shown in Fig.1. The solid lines are Gaussian fits with the width $2\sigma = 5.15$ (left) and 5.12 (right) detector pixels.

rays, respectively. In fact, the intrinsic width of the reflections in these long-range-ordered crystals is about $0.04 \mu\text{m}^{-1}$ [1,3], much smaller than their apparent width in Fig.2, i.e. the width is fully limited by the setup. This also explains the Gaussian rather than Lorentzian shape of the profiles.

To further enlighten the origin of the resolution limitation, Fig.3 presents a sketch of the x-ray optics in the present experiment. X-rays are focused at the detector creating an image of the x-ray source (the electron beam in the synchrotron). The smallest possible size of the direct and diffracted beams is then given by the size of the source [typically about $100 \mu\text{m}$ (RMS) to $300 \mu\text{m}$ (Peak) according to the ESRF] times the magnification factor $M = L_2/L_1$. The latter is equal to the ratio of the distances from the focusing element (F) to the detector plane (D) and the source, respectively. In the horizontal plane focusing is performed by the second crystal of the monochromator so that $L_1 = 33 \text{ m}$ and $L_2 = 24 \text{ m}$. Thus, in the horizontal direction $M = 0.73$ and the reflections cannot be made smaller than about $70 \mu\text{m}$. The achieved size of the reflections of $120 \mu\text{m}$ in Fig. 2 is clearly close to this ultimate limit suggesting (nearly) ideal optical elements and their perfect alignment. The construction in Fig.3 also explains why the physical size of the reflections on the detector does not depend on the x-ray energy. In the vertical direction focusing is performed by a bent silicon mirror located after the monochromator leading to a somewhat smaller magnification factor $M = 0.60$. However, the apparent vertical width of the reflections in Fig.1 is about 25% larger than that in the horizontal direction, which is presumably caused by stronger aberrations of the mirror.

To conclude, we have demonstrated that an ultimate resolution better than $1 \mu\text{m}^{-1}$ is achievable within the present setup at DUBBLE (with 10 keV x-rays). For a high-resolution scattering experiment the gas-filled detector (pixel size $255 \mu\text{m}$, apparent width of the reflections from the same set of samples $2\sigma \sim 4 \text{ pixels} = 1 \text{ mm}$ [2]) has a too poor resolution and must be replaced by another detector with an actual resolution in real space well beyond $100 \mu\text{m}$. Since the transverse resolution of a scattering scheme is inversely proportional to the transverse coherence length of the beam in the sample, Fig.3 also explains the bottleneck of the present setup at DUBBLE (note how much the Airy cone shrinks towards the sample position). We have recently applied for the beamtime at ID10A to investigate possibilities of further resolution improvement using compound refractive lenses with a shorter focal length. Since the sample-detector distance (setting up the relation between reciprocal space and actual real-space distances within the detector plane) is strictly limited by the size of the experimental hutch, the idea of the forthcoming experiment is to reduce the magnification factor M .

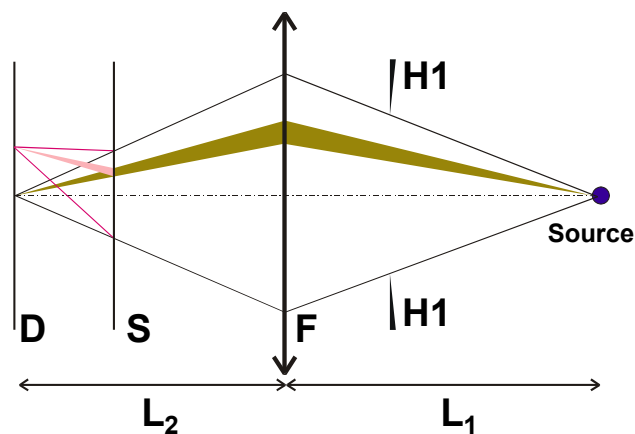


Figure 3. Sketch of beam focusing within the optical setup. **H1** denotes the entrance slits, **F** is a focusing element, **S** is the sample, and **D** is the detector plane. The shaded areas schematically denote Airy cones, where the radiation is coherent. Pink colour is used for a diffracted beam.

[1] A.V. Petukhov, I.P. Dolbnya, D.G.A.L. Aarts, G.J. Vroege, H.N.W. Lekkerkerker, Phys. Rev. Lett., **90**, 028304 (2003).

[2] A.V. Petukhov *et al.*, Phys. Rev. Lett., **88**, 208301 (2002).

[3] A.V. Petukhov I.P. Dolbnya, D.G.A.L. Aarts, G.J. Vroege, Phys. Rev. E, submitted (manuscript is available at <http://www.chem.uu.nl/fcc/drying>)